Research Square

Preprints are preliminary reports that have not undergone peer review.
They should not be considered conclusive, used to inform clinical practice,
or referenced by the media as validated information.

Repeated Oral Manganese Exposure-Associated Hepatorenal Injury in BALB/c Mice: Integrated Evidence from Tissue Accumulation, Redox Imbalance, Inflammation, and Histopathology

Olumayowa Kolawole Idowu
Osun State University
Yusrah Folashade Sanusi
Osun State University
Tajudeen Olamide Ajadi
Osun State University
Tolulope Ayodeji Oni
Osun State University
Adewale Emmanuel Ajibade
Adeleke University
Grace Ayobami Fajemidagba
Redeemers University
Abdullahi Abiodun Mohammed
a.mohammed@ur.ac.rw

University of Rwanda

Research Article

Keywords: BALB/c mice, manganese, hepatorenal injury, oxidative stress, inflammation, malondialdehyde, glutathione, histopathology, periodic acid–Schiff

Posted Date: September 7th, 2026

DOI: https://doi.org/10.21203/rs.3.rs-10739710/v1

License: This work is licensed under a Creative Commons Attribution 4.0 International License.
Read Full License

Additional Declarations: No competing interests reported.

Repeated Oral Manganese Exposure-Associated Hepatorenal Injury in BALB/c Mice: Integrated Evidence from Tissue Accumulation, Redox Imbalance, Inflammation, and Histopathology

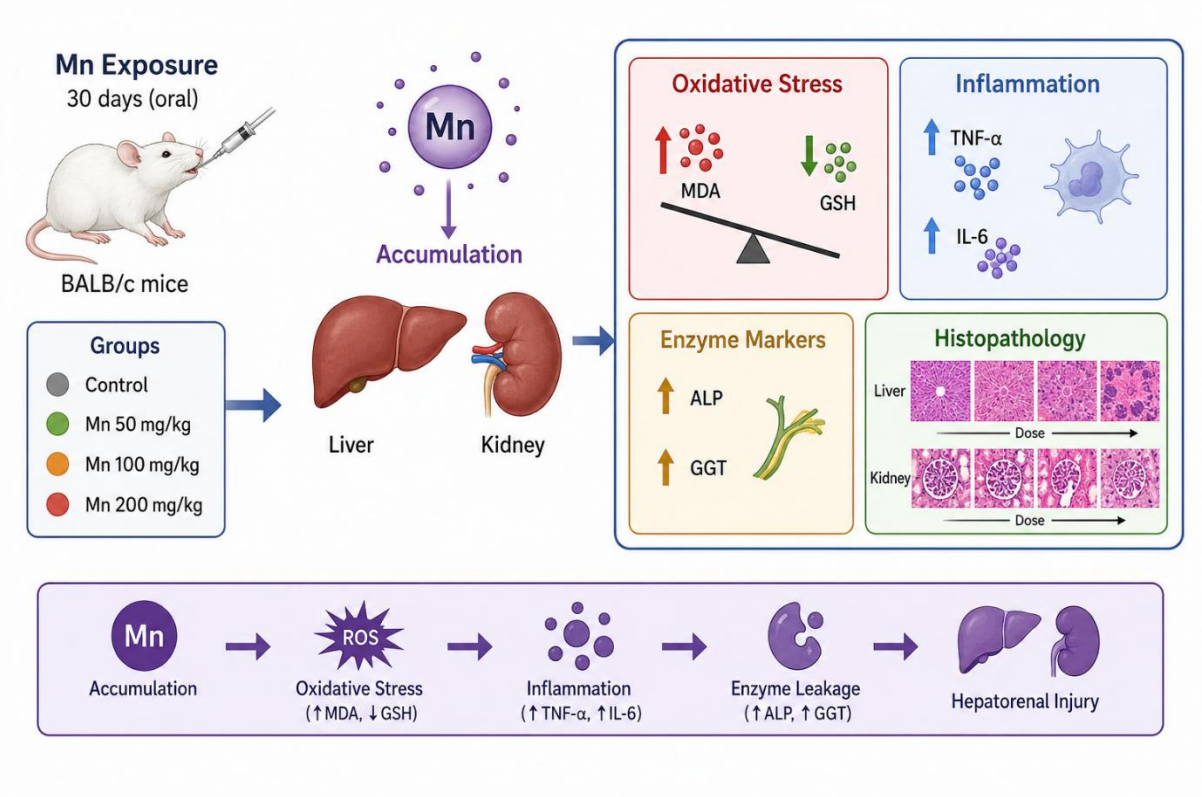
Abstract

Background: Manganese (Mn) is an essential trace element, but excessive exposure can result in tissue accumulation and toxicity. The liver and kidney are important organs in Mn homeostasis and elimination and may therefore be vulnerable to excessive Mn exposure. However, integrated evidence relating tissue Mn accumulation to redox imbalance, inflammatory responses, enzyme alterations, and structural injury remains limited. **Aim:** This study investigated the effects of repeated oral Mn exposure on hepatic and renal tissues in BALB/c mice. **Methods:** Thirty-two mice were randomly allocated to four groups (control, 50, 100, and 200 mg/kg Mn; n = 8/group) and treated orally for 30 days. Hepatic and renal Mn concentrations were quantified by inductively coupled plasma–optical emission spectrometry (ICP-OES). Serum alkaline phosphatase (ALP) and gamma-glutamyl transferase (GGT) activities; tissue malondialdehyde (MDA) and glutathione (GSH) concentrations; tissue tumour necrosis factor-alpha (TNF-α) and interleukin-6 (IL-6) concentrations; and hepatic and renal histopathology were evaluated. **Results:** Mn concentrations increased significantly in the livers and kidneys of exposed mice in a dose-dependent manner. Mn exposure was also associated with increased serum ALP and GGT activities, increased hepatic and renal MDA, increased TNF-α and IL-6 concentrations, and decreased GSH concentrations compared with controls ($p < 0.05$). H&E staining demonstrated progressive hepatocellular necrosis and cytoplasmic vacuolation, together with glomerular shrinkage and renal epithelial disruption. PAS staining showed progressively reduced hepatic staining intensity and attenuation of renal PAS reactivity, accompanied by structural alterations. **Conclusion:** Repeated oral Mn exposure was associated with dose-dependent hepatic and renal Mn accumulation, redox imbalance, inflammatory responses, enzyme alterations, and progressive histopathological injury. The findings support an association between tissue Mn burden and hepatorenal injury, while the molecular pathways underlying these effects require direct investigation.

Keywords: BALB/c mice; manganese; hepatorenal injury; oxidative stress; inflammation; malondialdehyde; glutathione; histopathology; periodic acid–Schiff

Graphical Abstract

Manganese accumulates in hepatic and renal tissues following repeated oral exposure, leading to oxidative stress, inflammatory activation, enzyme leakage, and progressive structural damage, culminating in dose-dependent hepatorenal toxicity.



Title: Manganese Accumulation Drives Oxidative Stress- and Inflammation-Mediated Hepatorenal Injury

Highlights

- Mn accumulated dose-dependently in the liver and kidney.
- Mn exposure disrupted tissue redox homeostasis.
- TNF-α and IL-6 increased in both organs.
- H&E and PAS showed progressive tissue injury.
- Integrated endpoints link Mn burden with organ injury.

Introduction

Manganese (Mn) is an essential trace element required for several physiological processes, including the activity of Mn-dependent enzymes and antioxidant defense. Because Mn homeostasis is tightly regulated, excessive exposure can result in tissue accumulation and adverse biological effects [1, 2]. The liver has a central role in Mn metabolism and biliary excretion, while the kidney contributes to elimination and is also vulnerable to toxic injury. Experimental evidence indicates that excessive Mn exposure can alter redox balance, inflammatory signaling, mitochondrial function, and tissue architecture.

Oxidative stress is an important component of experimental Mn toxicity. Increased lipid peroxidation and depletion of glutathione have been reported following excessive Mn exposure, consistent with impaired antioxidant capacity and cellular injury. In experimental liver injury, Mn has also been associated with activation of inflammatory signaling, including the cGAS–STING pathway, although such molecular responses depend on the experimental context [3]. Similarly, experimental studies have linked prolonged Mn exposure to alterations in hepatic antioxidant defenses, including the Nrf2 pathway [4]. These pathways provide biological context for the present findings but were not directly measured in this study.

The kidney is another potential target of Mn toxicity. Experimental Mn exposure has been associated with renal oxidative stress, mitochondrial impairment, and structural injury, including tubular and glomerular abnormalities [5].

Importantly, evidence of renal structural injury does not by itself establish impairment of renal filtration; functional biomarkers such as serum creatinine and blood urea nitrogen are therefore valuable complementary measures.

Although Mn toxicity has been extensively studied in relation to neurological effects, fewer experimental studies have integrated tissue Mn quantification with biochemical, inflammatory, enzymatic, H&E, and PAS assessments of both liver and kidney within the same experimental design. The present study therefore evaluated hepatic and renal Mn accumulation together with markers of lipid peroxidation, glutathione status, inflammatory cytokines, serum enzyme activities, and histopathological changes in BALB/c mice exposed to graded oral doses of Mn.

We hypothesized that repeated oral Mn exposure would produce dose-dependent hepatic and renal Mn accumulation associated with disruption of redox homeostasis, increased inflammatory responses, and progressive structural injury.

Materials and Methods

Chemical Procurement

Manganese (II) chloride tetrahydrate (purity 99%) was obtained from AK Scientific, Inc. (USA). Thiobarbituric acid (TBA) was obtained from Sigma-Aldrich (St. Louis, MO, USA). Phosphate-buffered saline (PBS) and other reagents required for the study were prepared from analytical-grade chemicals and authenticated at the Department of Pharmacology, Osogbo.

Ethical Statement

The study adhered to the National Institutes of Health recommendations for the care and use of laboratory animals and to the regulations of the Health Research Ethics Committee of the College of Health Sciences, Osun State University, Osogbo, Nigeria (Ethical Approval No. UNIOSUNHREC 2023/003D).

Animal Grouping and Treatment

Thirty-two adult male BALB/c mice were obtained from the Animal Holdings of Temmy Farms, Ogbomoso, Oyo State, Nigeria. The animals had free access to food and were allowed to acclimatize to the laboratory environment for two weeks before treatment. The experimental animals (20 – 22 g) were randomly allocated into four groups (n = 8/group): control, Mn 50, Mn 100, and Mn 200. The Mn-treated groups received 50, 100, or 200 mg/kg body weight (BW) Mn, respectively, whereas the control group received the standard diet and distilled water. Treatments were administered orally for 30 days. At the end of the exposure period, mice were deeply anesthetized by intraperitoneal administration of ketamine (100 mg/kg) and xylazine (10 mg/kg). Following confirmation of adequate anesthesia, the liver and kidneys were carefully excised through a midline abdominal incision, rinsed in ice-cold PBS to remove residual blood, gently blotted dry, and processed for biochemical and histopathological analyses.

Biochemical assays

Determination of Hepatic and Renal Manganese Concentrations

Liver and kidney Mn concentrations were determined using inductively coupled plasma–optical emission spectrometry (ICP-OES; Optima 8000, PerkinElmer, USA) following acid digestion as previously described by Dodd et al. (2005). Calibration curves were prepared from serial dilutions of certified single-element Mn standards, and multi-element quality-control standards were used to assess calibration accuracy and analytical precision. Procedural blanks and quality-control samples were analyzed after every 10 samples to monitor instrument performance. Standards, blanks, and quality-control samples were prepared in the same acid matrix as the tissue digests.

Briefly, tissue samples were digested in a mixture of 20% perchloric acid and 80% nitric acid and diluted to a final volume of 500 µL with 0.5% nitric acid. Instrument operating conditions included an RF power of 1200 W, sample uptake rate of 1.2 mL/min, argon gas pressure of 100 psi, and nebulizer pressure of 36 psi. Each sample analysis was preceded and followed by a 4-min rinse with the digestion solution to minimize carryover. Results were expressed as µg Mn/g wet tissue [6, 7].

Serum ALP and GGT Activities

Serum alkaline phosphatase (ALP) and gamma-glutamyl transferase (GGT) activities were determined using commercially available colorimetric enzyme activity assay kits (Elabscience, China; ALP Cat. No. E-BC-K091-S; GGT Cat. No. E-BC-K126-M), according to the manufacturer's instructions. These were enzyme activity assays rather than ELISA procedures. ALP activity was determined by the kinetic colorimetric method based on hydrolysis of p-nitrophenyl phosphate (pNPP) to p-nitrophenol under alkaline conditions. The rate of p-nitrophenol formation was monitored spectrophotometrically at 405 nm, and enzyme activity was expressed as IU/L.

GGT activity was determined using a kinetic enzymatic method in which L-γ-glutamyl-3-carboxy-4-nitroanilide served as the γ-glutamyl donor substrate and glycylglycine as the acceptor substrate. The reaction product was monitored spectrophotometrically at 405 nm, and enzyme activity was expressed as IU/L. Assays were performed according to the manufacturer's instructions and standardized to the stated analytical procedure.

Measurement of MDA and GSH

MDA and GSH levels were determined using established procedures [8, 9]. Briefly, liver and kidney tissue samples were weighed, homogenized in 0.1 M phosphate buffer (pH 7.4), and centrifuged at 3000 rpm for 15 min at 4 °C. The resulting supernatants were used for biochemical analyses. GSH was measured using Ellman's reagent (5,5′-dithiobis-(2-nitrobenzoic acid), DTNB), with absorbance measured at 412 nm. MDA was determined using the thiobarbituric acid reactive substances (TBARS) assay following reaction with TBA, with absorbance measured at 532 nm using a UV-1800 spectrophotometer (Shimadzu Corporation, Kyoto, Japan). Concentrations were calculated using the relevant molar extinction coefficients and expressed as μmol/mL.

Measurement of TNF-α and IL-6

Liver and kidney tissue samples were weighed, homogenized in ice-cold PBS (pH 7.4) containing protease inhibitors, and centrifuged at 10,000 × g for 15 min at 4 °C. Supernatants were collected for cytokine analysis. TNF-α and IL-6 concentrations were quantified using mouse ELISA kits (Elabscience, China; TNF-α Cat. No. E-EL-M3063; IL-6 Cat. No. E-EL-M0044), according to the manufacturer's instructions. Standards and samples were assayed in duplicate with blank and quality-control wells. Absorbance was measured at 450 nm using a SpectraMax Plus 384 microplate reader (Molecular Devices, USA), and concentrations were calculated from standard curves and expressed as pg/mL.

Histopathology

Liver and kidney tissues were trimmed of surrounding connective tissue and fixed in 10% neutral buffered formalin at a fixative-to-tissue ratio of approximately 10–20:1 for 24–48 h at room temperature [10]. Tissues were subsequently rinsed, dehydrated through graded ethanol, cleared in xylene, infiltrated with molten paraffin wax (56–60 °C), embedded, and sectioned at 4–6 μm using a Roundfin RD-485 rotary microtome (Roundfin Technology Co., Ltd., China). Sections were mounted on positively charged glass slides and dried at 60 °C for 30–60 min. For H&E staining, sections were deparaffinized, rehydrated through graded ethanol to distilled water, stained with hematoxylin, differentiated and blued as required, counterstained with eosin, dehydrated, cleared in xylene, and mounted with a resinous medium.

For PAS staining without diastase digestion, deparaffinized and rehydrated sections were oxidized in 0.5–1% periodic acid for 5–10 min, rinsed, treated with Schiff reagent for 10–15 min, washed in running tap water, lightly counterstained with hematoxylin, dehydrated, cleared, and mounted. PAS staining was used to demonstrate glycogen and other carbohydrate-rich tissue components [10]. Images were captured at ×400 magnification using a light microscope (Biobase Biozone Co., Ltd., China). Quantitative assessment of PAS staining intensity was performed using ImageJ software (National Institutes of Health, Bethesda, MD, USA).

Statistical Analyses

Data were expressed as mean ± SEM. Differences among groups were analyzed using one-way analysis of variance (ANOVA), followed by Tukey's multiple-comparisons test. Statistical analyses were performed using GraphPad Prism, and $p < 0.05$ was considered statistically significant.

Results

Mn accumulation in the liver and kidney

Hepatic and renal Mn concentrations were significantly higher in all Mn-exposed groups than in the control group ($p < 0.05$; Fig. 1A, B). Tissue Mn accumulation increased progressively with increasing administered Mn dose, indicating a dose-related increase in Mn burden in both organs.

Mn exposure increased serum ALP and GGT activities

Serum ALP and GGT activities were significantly higher in Mn-exposed groups than in controls ($p < 0.05$), with progressively greater activities across the increasing Mn-dose groups (Fig. 1C, D).

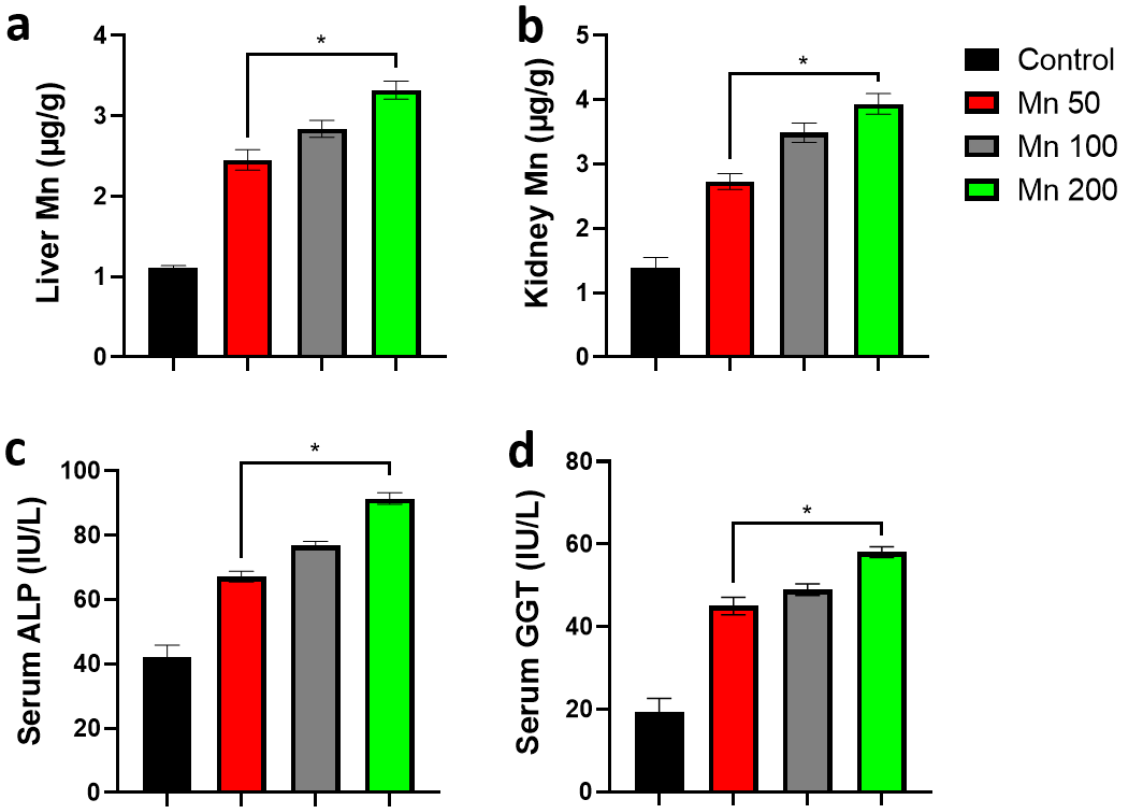


Fig. 1 Liver Mn concentration (A); Kidney Mn concentration (B); Serum ALP activity (C); Serum GGT activity (D). The data are shown as the mean ± S.E.M. at *: $p < 0.05$ compared with the control group (ALP: alkaline phosphatase, GGT: gamma-glutamyl transferase, Mn: manganese)

Mn exposure disrupted hepatic and renal redox homeostasis

Hepatic and renal MDA concentrations increased significantly in all Mn-exposed groups compared with controls ($p < 0.05$), with a dose-related pattern (Fig. 2A, B). Conversely, GSH concentrations were significantly reduced in both tissues following Mn exposure, with progressively lower values at higher Mn doses (Fig. 2C, D).

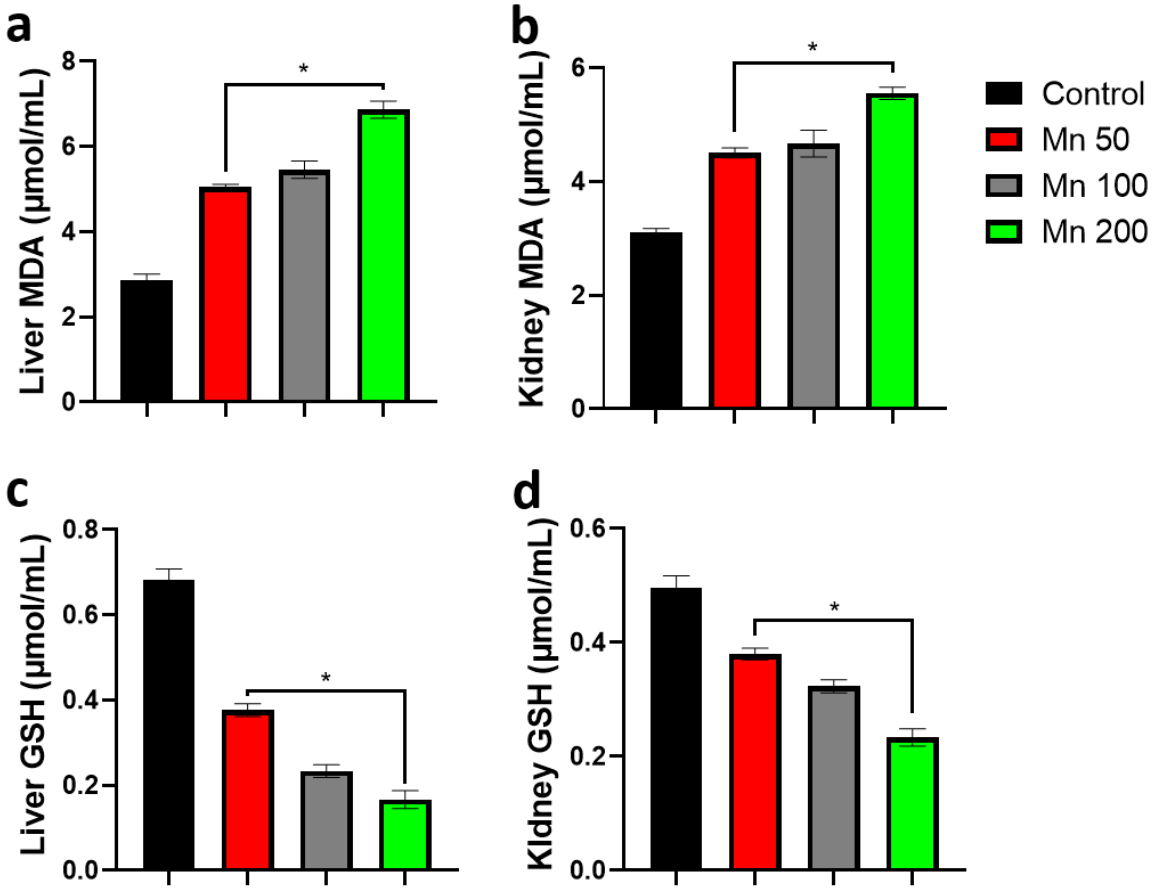


Fig. 2 Liver MDA level (A); Kidney MDA level (B); Liver GSH level (C); Kidney GSH level (D). The data are shown as the mean ± S.E.M.; *: $p < 0.05$ compared with the control group (GSH: glutathione, MDA: malondialdehyde, Mn: manganese)

Mn exposure increased tissue TNF-α and IL-6 concentrations

TNF-α concentrations were significantly increased in both liver and kidney tissues in Mn-treated groups compared with controls ($p < 0.05$), with a dose-related pattern (Fig. 3A, B). IL-6 concentrations were similarly elevated in both tissues following Mn exposure ($p < 0.05$; Fig. 3C, D).

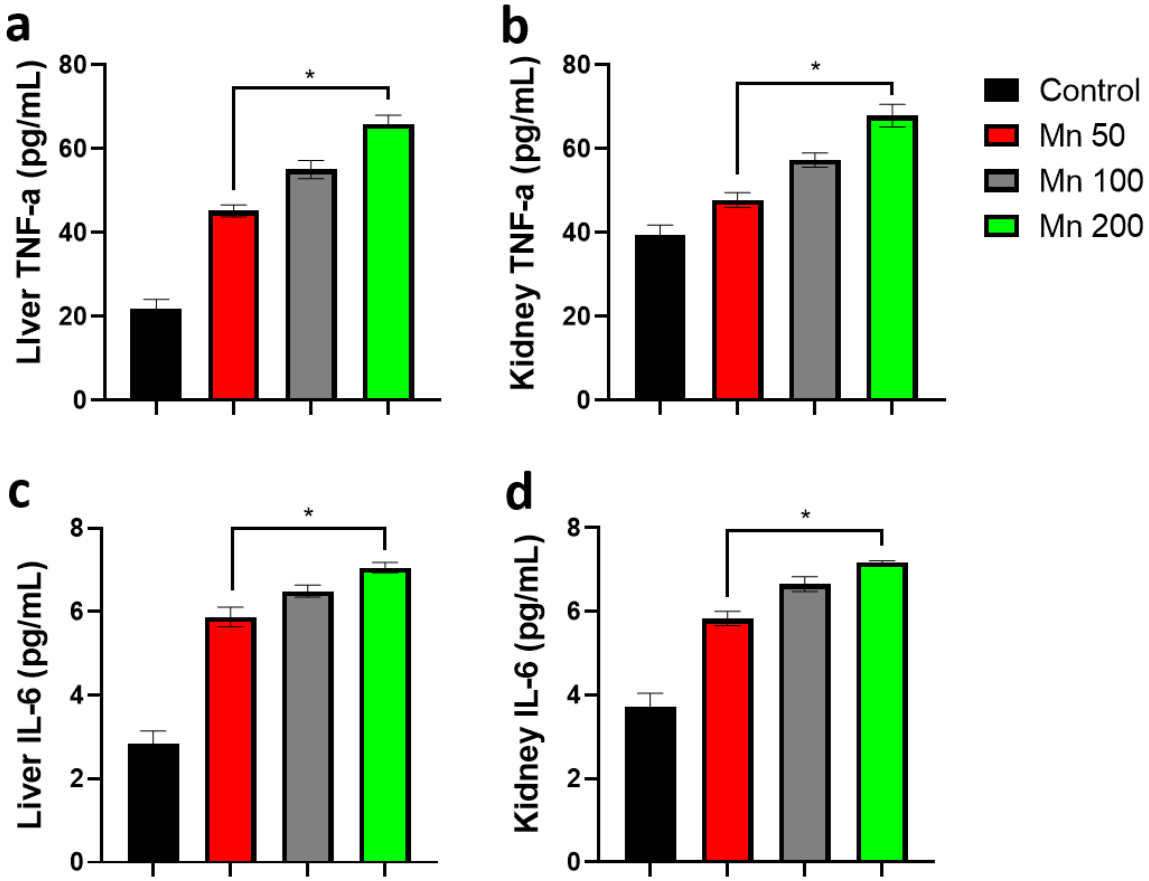


Fig. 3 Liver TNF-α level (A); Kidney TNF-α level (B); Liver IL-6 level (C); Kidney IL-6 level (D). The data are presented as the mean ± S.E.M.;* $p < 0.05$ compared with the control group (IL-6: Interleukin-6, Mn: manganese, TNF-α: Tumor Necrosis Factor-alpha).

Mn exposure induced hepatic and renal histoarchitectural alterations

H&E-stained liver sections from control mice showed preserved hepatic architecture, including intact hepatocytes and well-defined sinusoids (Fig. 4A). Mn 50-treated mice showed mild hepatocellular necrosis and cytoplasmic vacuolation (Fig. 4B). These changes were more pronounced in Mn 100-treated mice, which showed moderate necrosis and vacuolation (Fig. 4C), and were most extensive in Mn 200-treated mice, which exhibited severe hepatocellular necrosis and extensive cytoplasmic vacuolation (Fig. 4D). The previously described 'amyloid deposition' has been removed because H&E staining alone cannot establish amyloid identity.

Renal sections from control mice showed preserved glomerular and tubular architecture, including well-defined glomeruli and urinary spaces (Fig. 5A). Mild glomerular shrinkage, pyknotic nuclei, and irregular urinary spaces were observed in the Mn 50 group (Fig. 5B). These changes progressed to moderate glomerular shrinkage and distortion in the Mn 100 group (Fig. 5C), while the Mn 200 group showed severe glomerular shrinkage, irregular urinary spaces, epithelial disruption, karyolysis, and marked architectural deterioration (Fig. 5D).

PAS staining of liver sections showed intense staining in hepatocytes of control mice (Fig. 6A), whereas the Mn 50, Mn 100, and Mn 200 groups showed progressively reduced staining intensity (Fig. 6B–D). In kidney sections, control mice showed strong PAS reactivity in the glomerular basement membrane and proximal tubular brush borders (Fig. 7A). Mn exposure was associated with progressively attenuated PAS reactivity, collapse or distortion of Bowman's space, and disruption of glomerular architecture (Fig. 7B–D).

Quantitative analysis demonstrated a significant, dose-related reduction in hepatic and renal PAS staining intensity in Mn-treated groups compared with controls ($p < 0.05$; Fig. 8A, B).

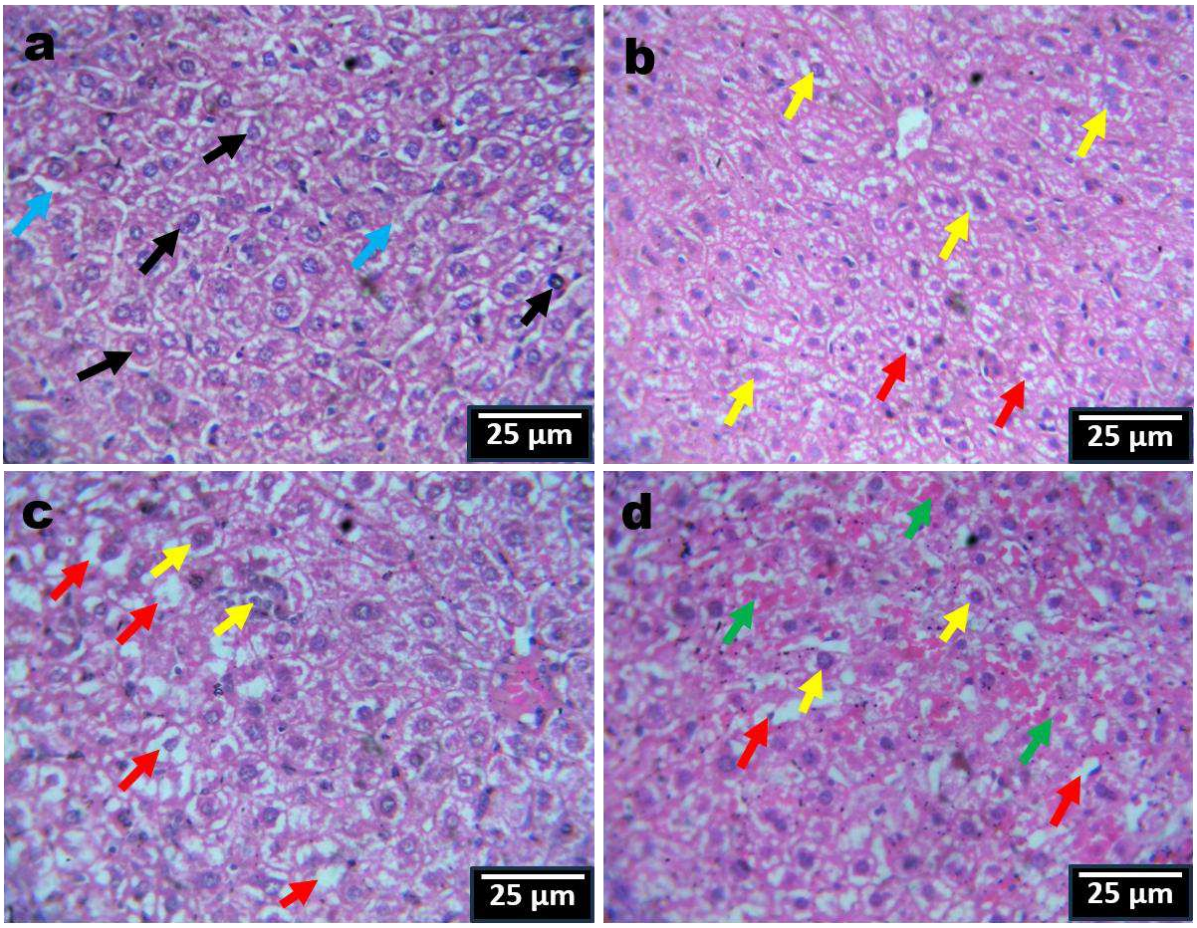


Fig. 4 Hematoxylin and eosin staining of mice liver tissue (x 400). Control (A), Mn 50 (B), Mn 100 (C), and Mn 200 (D). (Black arrows: normal hepatocytes, blue arrows: normal sinusoid, red arrows: vacuolation of the hepatocytes, yellow arrows: necrotic hepatic cells, green arrows: amyloid formation)

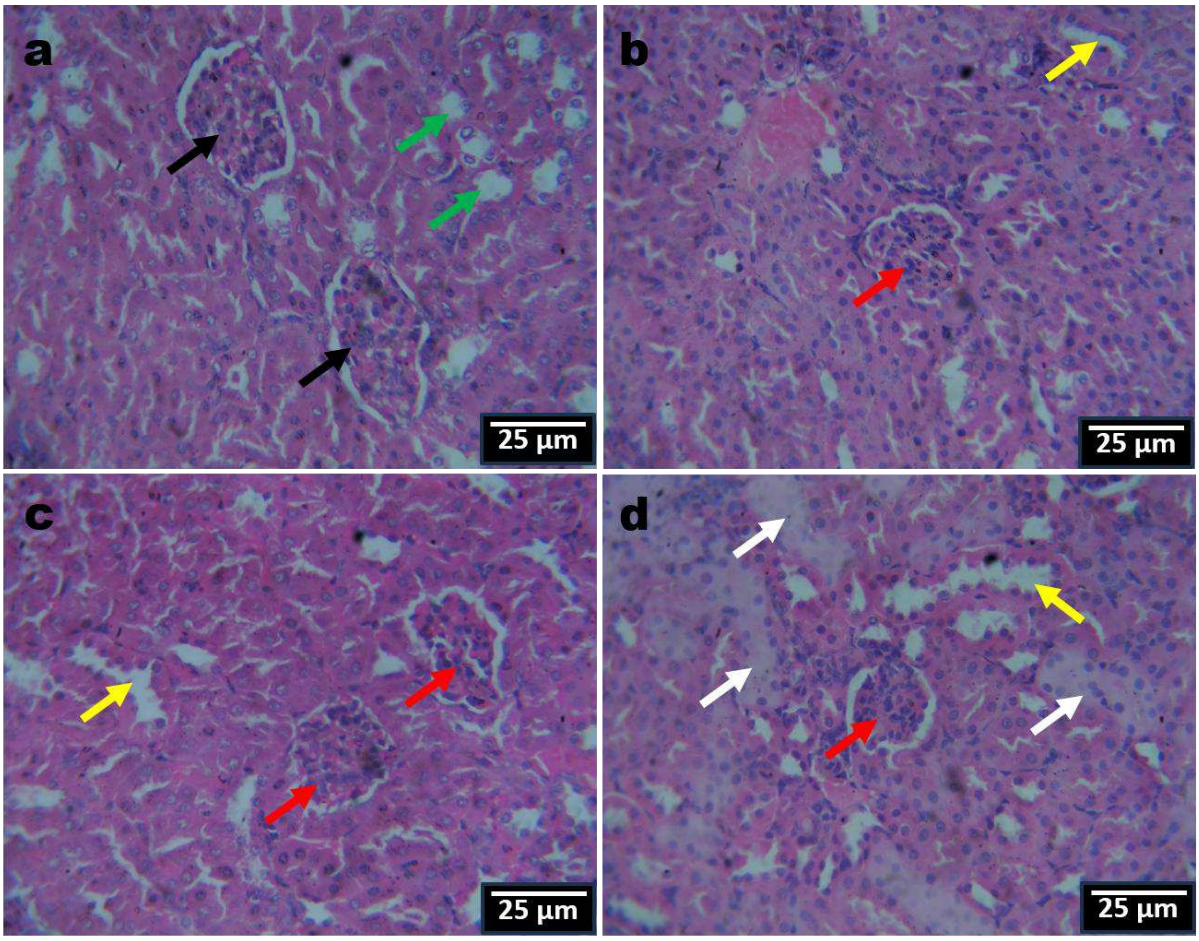


Fig. 5 Hematoxylin and eosin staining of mice kidney tissue (x 400). Control (A), Mn 50 (B), Mn 100 (C), and Mn 200 (D). (Black arrows: typical glomeruli with normal podocytes, green arrows: normal urinary space, red arrows: shrinking glomeruli with pyknotic cells, yellow arrows: irregular urinary space, white arrows: cellular karyolysis and disrupted epithelial tissue)

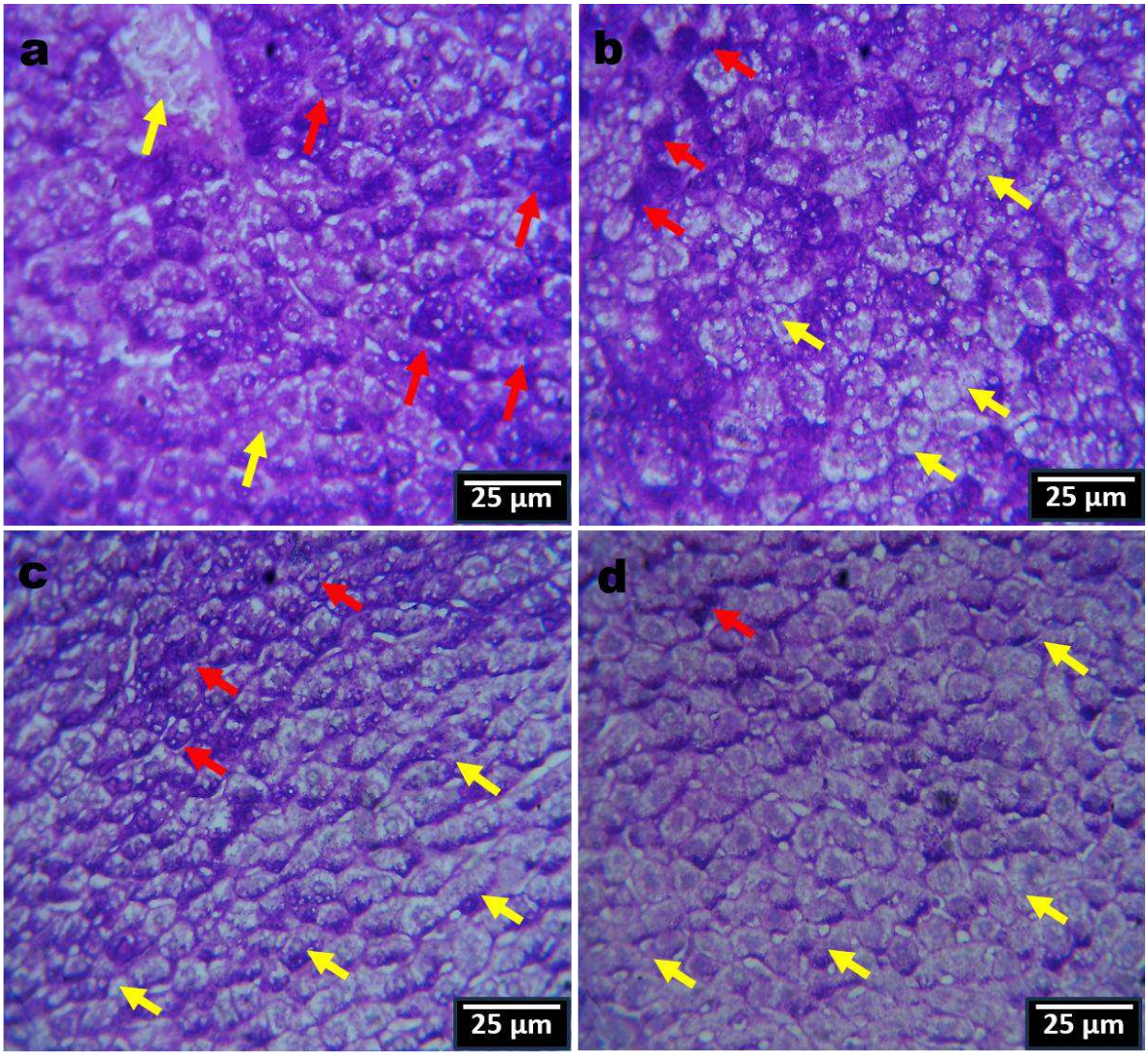


Fig. 6 Periodic acid schiff staining of mice liver tissue (x 400). Control (A), Mn 50 (B), Mn 100 (C), and Mn 200 (D). (Red arrows: deeply stained hepatocytes, yellow arrows: faintly stained hepatocytes)

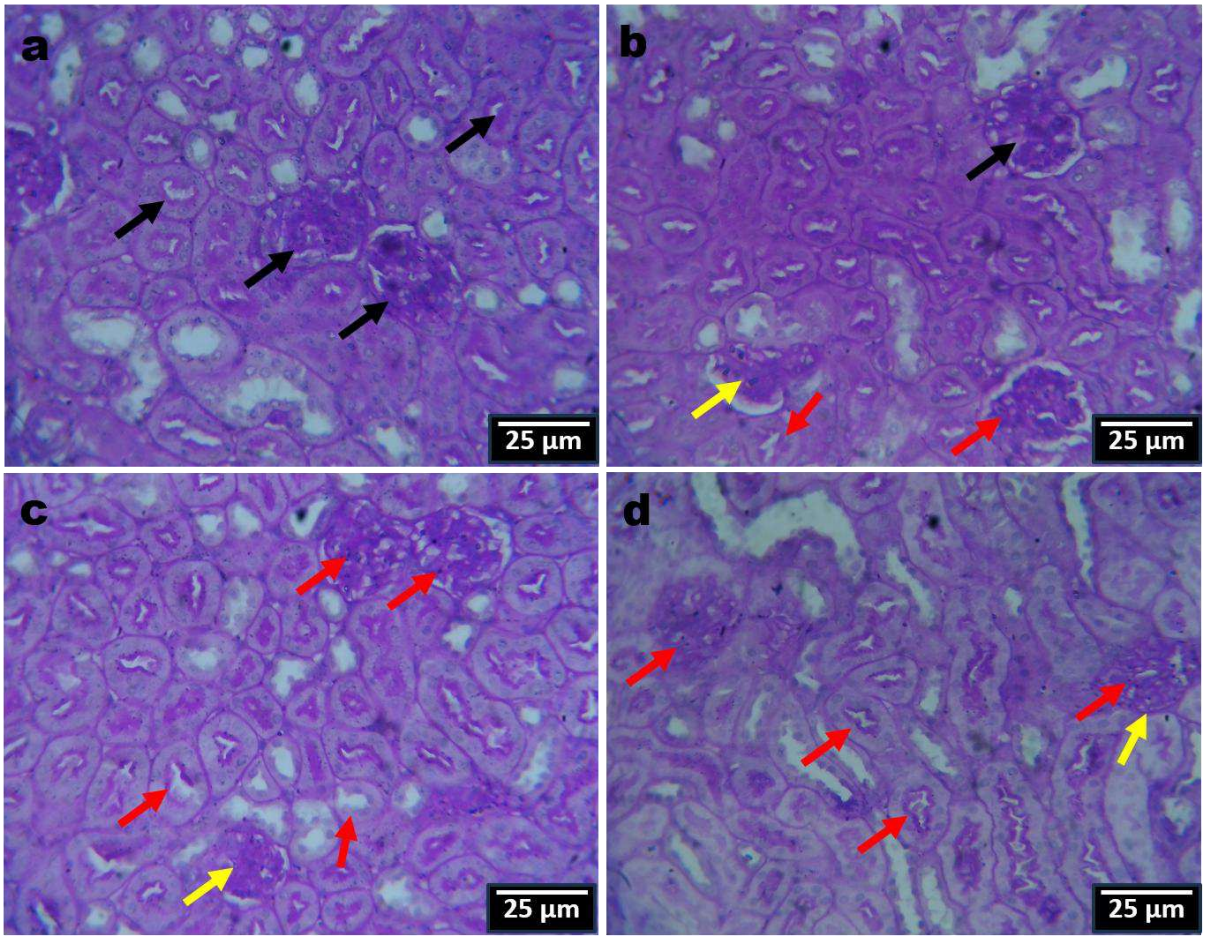


Fig. 7 Periodic acid Schiff staining of mice kidney tissue (x 400). Control (A), Mn 50 (B), Mn 100 (C), and Mn 200 (D). (Black arrows: deeply stained glomerular basement membrane and tubular brush borders, red arrows: faintly stained glomerular basement membrane and tubular brush borders, yellow arrows: collapsed Bowman's space and disrupted glomerulus)

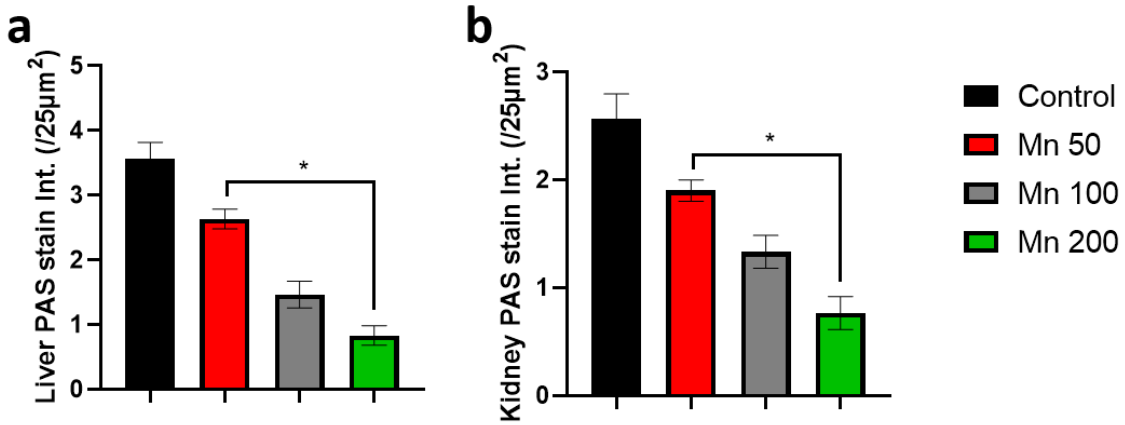


Fig. 8 Liver PAS stain intensity (A); Kidney PAS stain intensity (B). The data are shown as the mean ± S.E.M. at *: $p < 0.05$ compared with the control group (Mn: manganese, PAS: periodic acid–Schiff)

Discussion

The present study demonstrates an integrated pattern of hepatic and renal alterations following repeated oral Mn exposure. The dose-related increase in tissue Mn concentrations indicates that the administered exposure resulted in progressive Mn accumulation in both organs. This finding is consistent with the established role of the liver in Mn handling and biliary excretion and with evidence that Mn can accumulate in tissues following repeated exposure [1, 2].

The increases in serum ALP and GGT activities provide biochemical evidence of hepatic or hepatobiliary disturbance following Mn exposure [11]. These enzymes are commonly used as indicators of hepatobiliary injury, although their interpretation is not specific to a single cellular lesion. Because ALT and AST were not measured in the present study, the biochemical evidence of hepatic injury is interpreted in conjunction with the histopathological findings rather than as a complete assessment of hepatic function.

The simultaneous increase in MDA and decrease in GSH in liver and kidney tissues indicates disruption of redox homeostasis [12]. Increased MDA is consistent with enhanced lipid peroxidation, whereas reduced GSH suggests depletion of an important endogenous antioxidant reserve. Similar oxidative changes have been described in experimental Mn exposure, including studies reporting hepatic oxidative injury and altered antioxidant defenses [4]. The present study did not directly measure ROS generation, mitochondrial function, Nrf2 signaling, or antioxidant enzyme activities such as superoxide dismutase and catalase. Accordingly, the observed MDA/GSH pattern supports oxidative imbalance but does not establish a specific molecular pathway.

Mn exposure was also associated with increased tissue TNF-α and IL-6 concentrations [13]. These findings indicate an inflammatory response in both organs. Oxidative stress and inflammation can reinforce one another during toxicant-induced tissue injury; however, the present study cannot determine whether oxidative stress preceded inflammatory activation or whether a particular upstream inflammatory pathway mediated the response. Published experimental evidence implicates pathways such as NF-κB and cGAS–STING in inflammatory responses to cellular stress and Mn exposure, respectively, but these pathways were not directly assessed here [3].

Histopathological findings provide structural support for the biochemical alterations. The progressive hepatic necrosis and vacuolation and the renal glomerular and epithelial abnormalities became more pronounced with increasing Mn dose. These changes are consistent with experimental evidence of Mn-associated renal oxidative and mitochondrial injury [5]. The absence of quantitative lesion scoring in the present study means that the histopathological observations should be regarded primarily as descriptive evidence of structural injury.

Reduced PAS staining intensity in the liver is consistent with reduced detectable glycogen or other PAS-positive carbohydrate-containing material [14]. In the kidney, reduced PAS reactivity in glomerular basement membranes and tubular brush borders is consistent with alteration or loss of PAS-positive structures. However, because PAS staining without diastase digestion is not specific for glycogen, the hepatic findings should not be interpreted as definitive glycogen depletion without complementary biochemical or histochemical confirmation.

A limitation is that renal functional biomarkers, including serum creatinine and blood urea nitrogen, were not measured. Thus, the renal findings demonstrate structural and biochemical evidence of renal injury but do not establish the degree of functional impairment. Similarly, the study did not directly measure molecular signaling pathways proposed in the mechanistic framework. The integrated data therefore support an association in which increasing tissue Mn burden occurs alongside redox imbalance, inflammatory responses, and progressive structural injury, rather than proving a causal molecular sequence.

Hypothesized Mechanisms

Repeated oral Mn exposure is associated with hepatic and renal Mn accumulation, redox imbalance, inflammatory responses, biochemical alterations, and structural injury. Molecular pathways shown are proposed based on published evidence and were not directly measured in the present study.

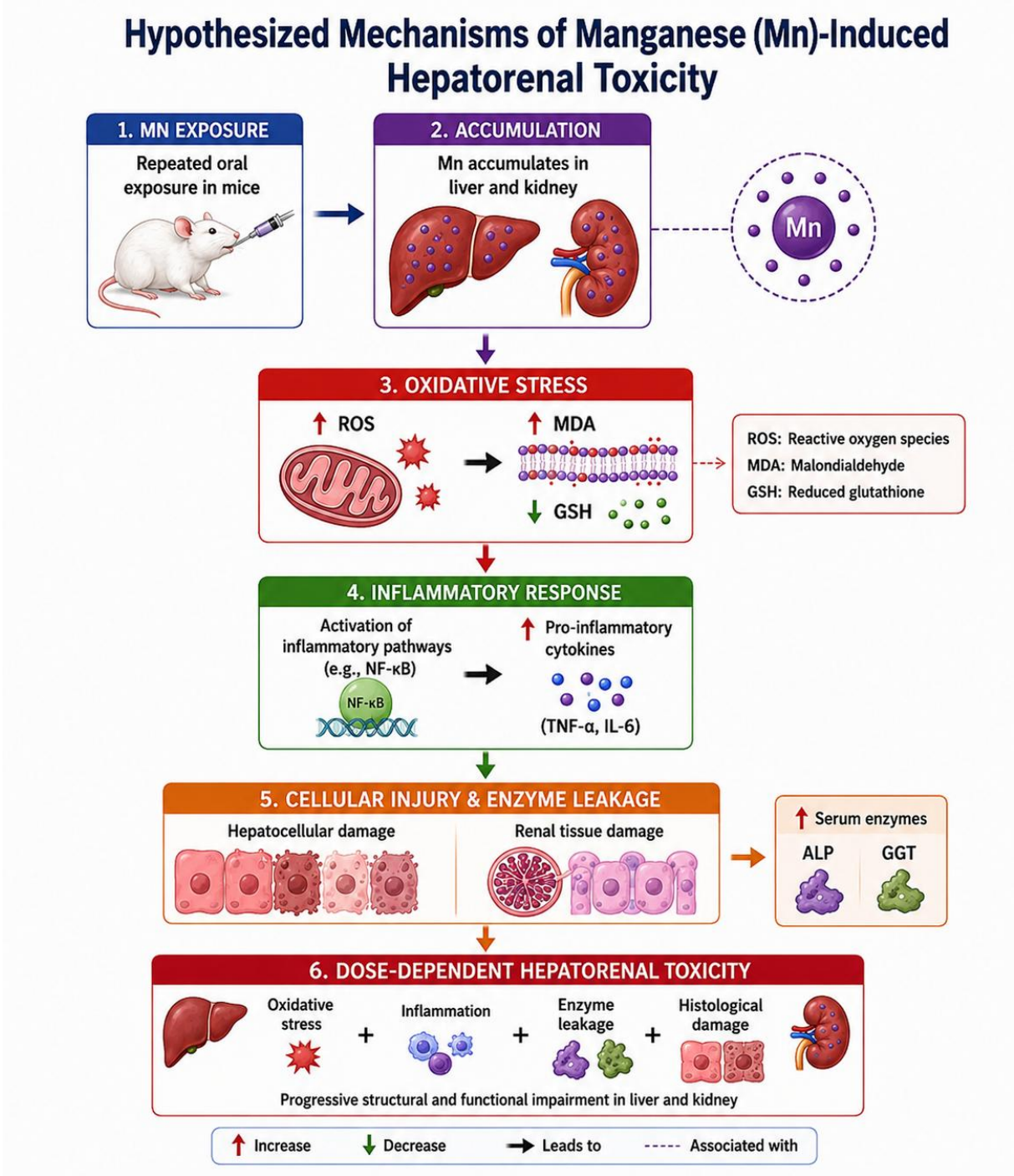


Fig. 10 Hypothesized mechanisms underlying manganese-induced hepatorenal toxicity

Conclusion

Repeated oral Mn exposure for 30 days produced dose-dependent accumulation of Mn in the liver and kidney of BALB/c mice and was associated with disruption of tissue redox homeostasis, increased inflammatory cytokines, elevated serum ALP and GGT activities, and progressive hepatic and renal histopathological alterations. The

concordance between tissue Mn accumulation and biochemical and structural changes supports a relationship between Mn burden and hepatorenal injury. However, the specific molecular pathways and the extent of functional renal impairment require further investigation.

Limitations

Although this study comprehensively characterized Mn-induced hepatorenal toxicity, it did not investigate the underlying molecular signaling pathways or assess organ-specific functional biomarkers. Future studies integrating mechanistic and functional analyses are warranted to further elucidate the pathways driving Mn-induced liver and kidney injury.

Author Contributions

OKI: conceptualization, methodology, investigation, formal analysis, data curation, visualization, supervision, writing – original draft, writing – review and editing. **YFS:** conceptualization, methodology, project administration, resources, writing – original draft. **TOA:** investigation, formal analysis, data curation, writing – review and editing. **TAO:** investigation, formal analysis, data curation, writing – review and editing. **AEA:** investigation, formal analysis, visualization, writing – review and editing. **GAF:** investigation, formal analysis, visualization, writing – review and editing. **AAM:** investigation, formal analysis, visualization, supervision, writing – review and editing. All authors read and approved the final manuscript.

Funding

No financial support was received during the study and the writing of this manuscript.

Competing Interests

There are no competing interests that are relevant to the paper that need to be disclosed.

Data Availability

The data generated and/or assessed in this study are available to the public via the Zenodo repository at https://doi.org/10.5281/zenodo.21972354.

References

1. Chen P, Bornhorst J, Aschner M (2018) Manganese metabolism in humans. Front Biosci (Landmark Ed) 23:1655–1679. https://doi.org/10.2741/4665

2. Erikson KM, Aschner M (2019) Manganese: its role in disease and health. Metal Ions Life Sci 19:253–266. https://doi.org/10.1515/9783110527872-010

3. Saimaier K, Han S, Lv J et al (2024) Manganese exacerbates ConA-induced liver inflammation via the cGAS-STING signaling pathway. Inflammation 47:333–345. https://doi.org/10.1007/s10753-023-01912-4

4. Wang X, Shen X, Chen L et al (2021) Hepatic oxidative damage and Nrf2 pathway protein changes in rats following long-term manganese exposure. Toxicol Ind Health 37:251–259. https://doi.org/10.1177/0748233721993311

5. Niknahad AM, Ommati MM, Farshad O et al (2020) Manganese-induced nephrotoxicity is mediated through oxidative stress and mitochondrial impairment. J Ren Hepat Disord 4(2):1–10. https://doi.org/10.15586/jrenhep.2020.66

6. Dodd CA, Ward DL, Klein BG (2005) Basal ganglia accumulation and motor assessment following manganese chloride exposure in the C57BL/6 mouse. Int J Toxicol 24:389–397. https://doi.org/10.1080/10915810500366500

7. Lin W, Vann DR, Doulias PT et al (2017) Hepatic metal ion transporter ZIP8 regulates manganese homeostasis and manganese-dependent enzyme activity. J Clin Invest 127:2407–2417. https://doi.org/10.1172/JCI90896

8. Sedlak J, Lindsay RH (1968) Estimation of total, protein-bound, and nonprotein sulfhydryl groups in tissue with Ellman's reagent. Anal Biochem 25:192–205. https://doi.org/10.1016/0003-2697(68)90092-4

9. Karatas F, Karatepe M, Baysar AH (2002) Determination of free malondialdehyde in human serum by high-performance liquid chromatography. Anal Biochem 311(1):76–79. https://doi.org/10.1016/S0003-2697(02)00387-1

10. Bancroft JD, Gamble M (2008) Theory and practice of histological techniques, 6th edn. Churchill Livingstone Elsevier11. Adetunji AG, Obeng-Gyasi E. Investigating the interplay of toxic metals and essential elements in liver disease. International Journal of Environmental Research and Public Health. 2024 Jun 12;21(6):762. https://doi.org/10.3390/ijerph21060762

11. Adetunji AG, Obeng-Gyasi E. Investigating the interplay of toxic metals and essential elements in liver disease. International Journal of Environmental Research and Public Health. 2024 Jun 12;21(6):762. https://doi.org/10.3390/ijerph21060762

12. Abdeen A, Abdelkader A, Elgazzar D, Aboubakr M, Abdulah OA, Shoghy K, Abdel-Daim M, El-Serehy HA, Najda A, El-Mleeh A. Coenzyme Q10 supplementation mitigates piroxicam-induced oxidative injury and apoptotic pathways in the stomach, liver, and kidney. Biomedicine & Pharmacotherapy. 2020 Oct 1;130:110627. https://doi.org/10.1016/j.biopha.2020.110627

13. Liang DY, Peng JC, Xie BY, Qin WX, Aschner M, Ou SY, Jiang YM. Effects of combined exposure of manganese and iron on serum inflammatory factor levels among workers. Human & Experimental Toxicology. 2024 Oct 9;43:09603271241293112. https://doi.org/10.1177/09603271241293112

14. Babcock MB, Cardell Jr RR. Hepatic glycogen patterns in fasted and fed rats. American Journal of Anatomy. 1974 Jul;140(3):299-337. https://doi.org/10.1002/aja.1001400302